

Supporting Information for:  
Validation of a transcriptome-based  
assay for classifying cancers of  
unknown primary origin

## Supplementary Methods

### RNA Normalization

Raw transcript level counts were generated with Kallisto (v0.44.0). Transcripts were quantile-normalized with 100 quantiles to account for GC bias and transcript length.

```
factor = gc_content
global_median = median(expression_vector)
quantile_bins = expression.groupby(factor)
for bin in quantile_bins:
    bin_median = median(bin)
    scaling_factor = bin_median/global_median
    expression = bin/scaling_factor
```

The library size normalization consists of a fit and transform step. During the fit step, a cohort of training data is used to calculate the transcript-wise geometric expression. During the transform step, the learned geometric means are used to calculate a per-sample scaling factor based on the median of the ratio of sample expression to geometric mean of expression.

fit:

```
expression_matrix = [samples x transcripts matrix]
geomean = {}
for transcript in expression_matrix:
    geomean[transcript] = geomean(transcript)
```

transform:

```
for sample in expression_matrix:
    scaling_factor = median(sample/geomean)
    sample = sample/scaling_factor
```

### Batch Correction

The Tempus TO algorithm was trained on a cohort of RNA samples acquired on two different assay versions. Prior to Oct. 2020, samples were run on the version one RNA assay (RS.v1) whereas samples processed after Oct. 2020 were run on version two of the RNA assay (RS.v2). While the differences between assay versions were small in most cases, a simple batch correction method was developed and applied to further reduce differences between assay versions. This method, dubbed “cognizant correction”, leverages ~500 paired samples that were run on both platforms to match the means and variances of normalized expression. Cognizant correction learns per-gene linear transformations to match the RS.v2 data to the RS.v1 data. The slope and intercept coefficients were fitted independently for each gene, using the

corresponding normalized expression data, to match their distributions while accounting for pair-membership metadata. Cognizant correction optimizes coefficients by minimizing a loss function based on a weighted version of the Kullback-Leibler divergence that can account for subset-membership metadata, in this case the pairing information.

## Supplementary Figures and Tables

**Figure S1:** Validation of expression with orthogonal qPCR assay. Mean delta CT values for each sample and gene were normalized to the mean of the average CT values of two the housekeeping genes *AAMP* and *CANX* for that sample. Expression data were normalized to control for library size, GC content and transcript length before being log-transformed.

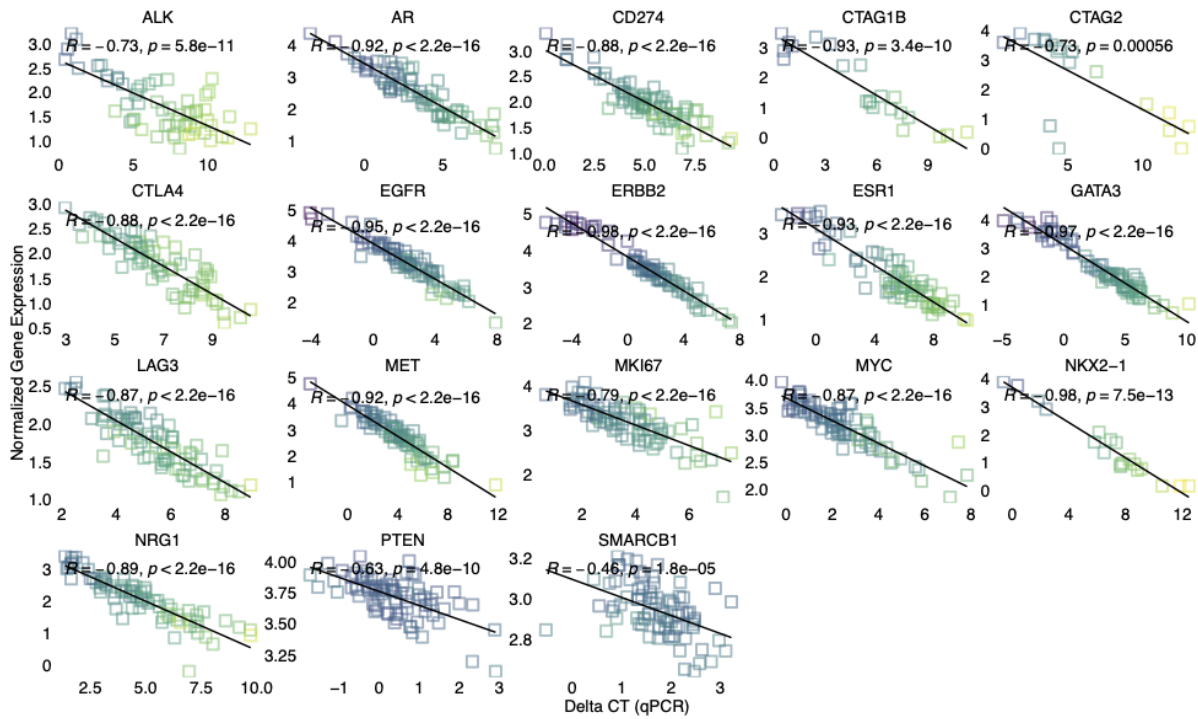




**Figure S3.** Model-predicted (Y-axis) and assigned (X-axis) subtype labels of Tempus samples are evaluated using a confusion matrix.

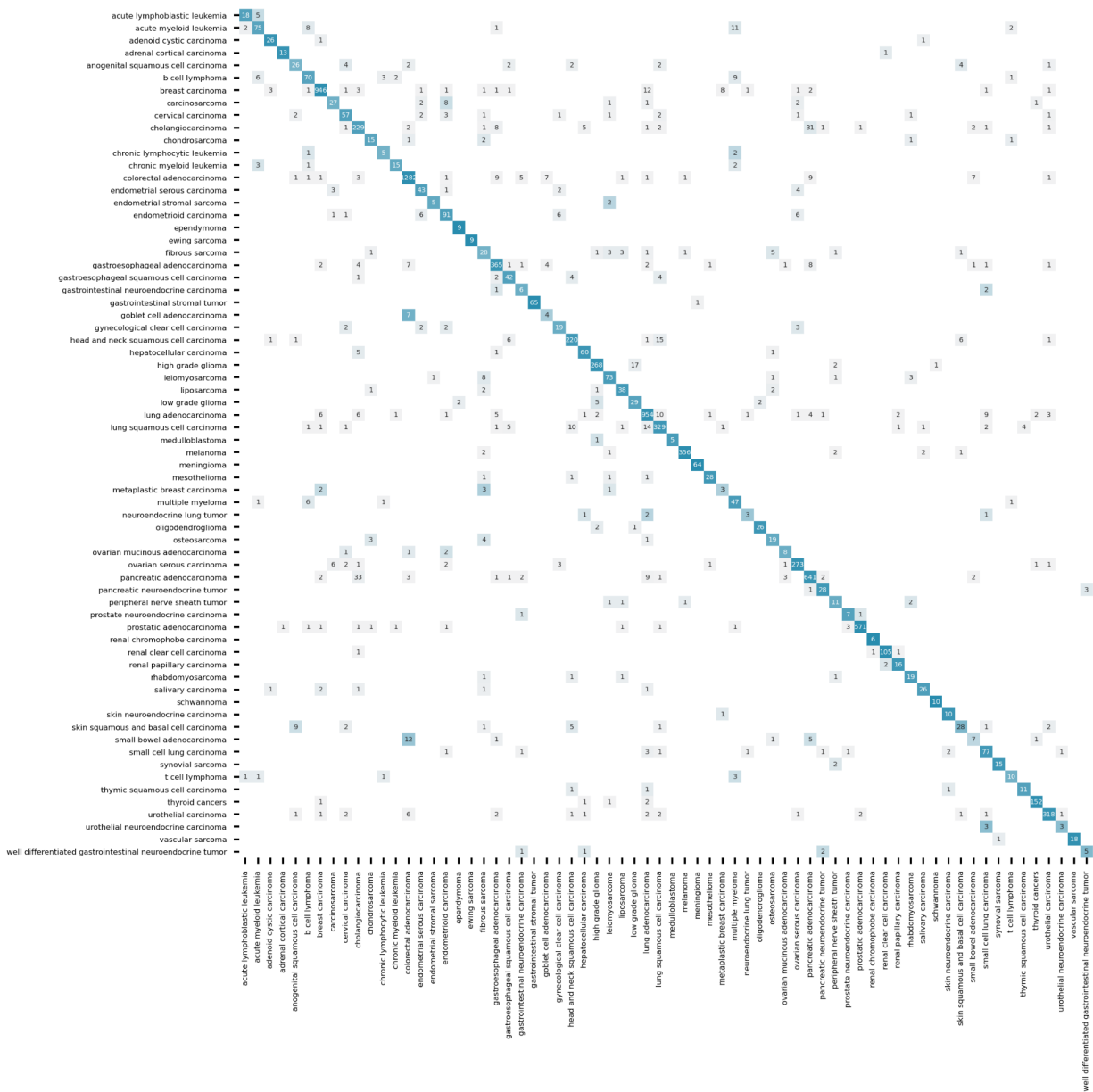






**Table S1.** Tissue site distribution of training and validation sets.

(See full table in supporting spreadsheet.)

**Table S2.** Subtype distribution of training and validation sets.

(See full table in supporting spreadsheet.)

**Table S3.** Model performance for each cancer subtype and each subcohort (validation, prospective, and retrospective).

(See full table in supporting spreadsheet.)

**Table S4.** A histology-level mapping between TCGA and Tempus TO subtypes is provided.

(See full table in supporting spreadsheet.)

**Table S5.** A crosswalk was constructed to align the subtypes herein to the types in the TCGA dataset.

(See full table in supporting spreadsheet.)

**Table S6.** Model performance on the total validation set and two sub-cohorts (prospective samples that were sequenced after model development and retrospective samples that were randomly held out from model training). Fisher’s exact test ( $p=0.621$ ) was used to assess significance between the cohorts (prospective vs retrospective) and prediction status (correct vs incorrect). Detailed results per subtype are shown in **Table S3**. In the smaller prospective cohort, some subtypes were not observed and were thus excluded from the mean sensitivity calculation.

	<b>Validation</b>	<b>Prospective</b>	<b>Retrospective</b>
Sample Size	9210	2483	6727
Accuracy	91.1%	90.8%	91.2%
Top 3 Accuracy	97.5%	97.6%	97.5%
Mean Sensitivity	80.0%	76.8%	81.0%

**Table S7.** Model performance stratified by tumor purity.

<b>Tumor Purity</b>	<b>N</b>	<b>Sensitivity</b>
0.0 < x <= 10.0	41	80.5%
10.0 < x <= 20.0	734	89.0%
20.0 < x <= 30.0	626	90.1%
30.0 < x <= 40.0	1229	92.9%
40.0 < x <= 50.0	1415	93.0%
50.0 < x <= 60.0	1340	92.8%
60.0 < x <= 70.0	1332	93.0%
70.0 < x <= 80.0	1531	89.9%
80.0 < x <= 90.0	713	90.3%
90.0 < x <= 100.0	1	100.0%

**Table S8.** Model performance stratified by imputed metastatic status.

<b>Sample Type</b>	<b>Count</b>	<b>Accuracy</b>
Ambiguous - Lymph Node Sample	652	91.2%
Evidence Against Primary Sample	359	89.5%
Possible Metastatic Sample	1796	88.0%
Possible Primary Sample	3041	93.5%
Possible Recurrent Sample	335	91.0%
Unknown	2204	90.6%



**Table S9.** Model performance on TCGA data is summarized via several performance metrics and descriptive statistics.

<b>Metric</b>	<b>Value</b>
Sample Size	9976
Accuracy	84.3%
Top 3 Accuracy	91.4%
Mean Sensitivity	85.2%

**Table S10.** Per-subtype model performance on TCGA is summarized.

	<b>observed</b>	<b>tp</b>	<b>sensitivity</b>
acute lymphoblastic leukemia	0	0	
acute myeloid leukemia	0	0	
adenoid cystic carcinoma	0	0	
adrenal cortical carcinoma	81	72	88.9%
anogenital squamous cell carcinoma	0	0	
b cell lymphoma	41	36	87.8%
breast carcinoma	1206	1129	93.6%
carcinosarcoma	12	11	91.7%
cervical carcinoma	306	126	41.2%
cholangiocarcinoma	47	30	63.8%
chondrosarcoma	0	0	
chronic lymphocytic leukemia	0	0	
chronic myeloid leukemia	0	0	
colorectal adenocarcinoma	441	392	88.9%
endometrial serous carcinoma	78	35	44.9%
endometrial stromal sarcoma	0	0	
endometrioid carcinoma	119	84	70.6%
ependymoma	0	0	
ewing sarcoma	0	0	
fibrous sarcoma	75	55	73.3%
gastroesophageal adenocarcinoma	485	450	92.8%
gastroesophageal squamous cell carcinoma	87	34	39.1%
gastrointestinal neuroendocrine carcinoma	0	0	
gastrointestinal stromal tumor	0	0	
goblet cell adenocarcinoma	0	0	
gynecological clear cell carcinoma	0	0	
head and neck squamous cell carcinoma	564	485	86.0%
hepatocellular carcinoma	415	362	87.2%
high grade glioma	160	139	86.9%
leiomyosarcoma	108	75	69.4%
liposarcoma	61	44	72.1%
low grade glioma	340	251	73.8%
lung adenocarcinoma	581	513	88.3%
lung squamous cell carcinoma	562	438	77.9%
medulloblastoma	0	0	
melanoma	573	521	90.9%
meningioma	0	0	

mesothelioma	86	77	89.5%
metaplastic breast carcinoma	15	7	46.7%
multiple myeloma	0	0	
neuroendocrine lung tumor	0	0	
oligodendroglioma	203	101	49.8%
osteosarcoma	0	0	
ovarian mucinous adenocarcinoma	0	0	
ovarian serous carcinoma	380	350	92.1%
pancreatic adenocarcinoma	177	165	93.2%
pancreatic neuroendocrine tumor	0	0	
peripheral nerve sheath tumor	10	5	50.0%
prostate neuroendocrine carcinoma	0	0	
prostatic adenocarcinoma	570	520	91.2%
renal chromophobe carcinoma	92	86	93.5%
renal clear cell carcinoma	616	470	76.3%
renal papillary carcinoma	329	271	82.4%
rhabdomyosarcoma	0	0	
salivary carcinoma	0	0	
schwannoma	0	0	
skin neuroendocrine carcinoma	0	0	
skin squamous and basal cell carcinoma	2	0	0.0%
small bowel adenocarcinoma	0	0	
small cell lung carcinoma	0	0	
synovial sarcoma	10	8	80.0%
t cell lymphoma	0	0	
thymic squamous cell carcinoma	128	112	87.5%
thyroid cancers	581	553	95.2%
urothelial carcinoma	435	404	92.9%
urothelial neuroendocrine carcinoma	0	0	
vascular sarcoma	0	0	
well differentiated gastrointestinal neuroendocrine tumor	0	0	

**Table S11.** Observed somatic mutation frequency (in the labeled and CUP cohorts) and Fisher p-values for the DNA variant analysis.

(See full table in supporting spreadsheet.)